Data Description for *Linear Axis Testbed – Rail Degradation Experiment 01*

Summary

This document provides details on the files available in the dataset titled “Linear Axis Testbed – Rail Degradation Experiment 01”. A rail of a linear axis testbed was degraded with data collected from an inertial measurement unit (IMU) at each stage of degradation. The data can be used to tracking the changing error motions, as described in Vogl et al.

Linear Axis Testbed

As seen in Figure 1, a linear axis testbed was designed for data collection with an inertial measurement unit (IMU). A custom IMU was developed that is about 9 cm long and contains a triaxial accelerometer and a triaxial rate gyroscope. The bandwidths and noise properties of these sensors are shown in Table 1. The testbed includes a linear axis, the IMU (for ‘Sensor Box Data’), and a commercial laser-based system for measuring the geometric error motions of the axis (for ‘Reference Data’). The trucks and rails of the testbed can be mechanically degraded for testing of IMU-based metrics to monitor degradation levels. For any state of the system, the laser-based metrology system measures the motion of the carriage with respect to the base of the linear axis, and the IMU measures the changes in the inertial motion of the carriage. The laser-based system is used to verify the IMU-based results over the travel length of 0.322 m with standard uncertainties of 0.7 µm and 3.0 µrad, respectively.

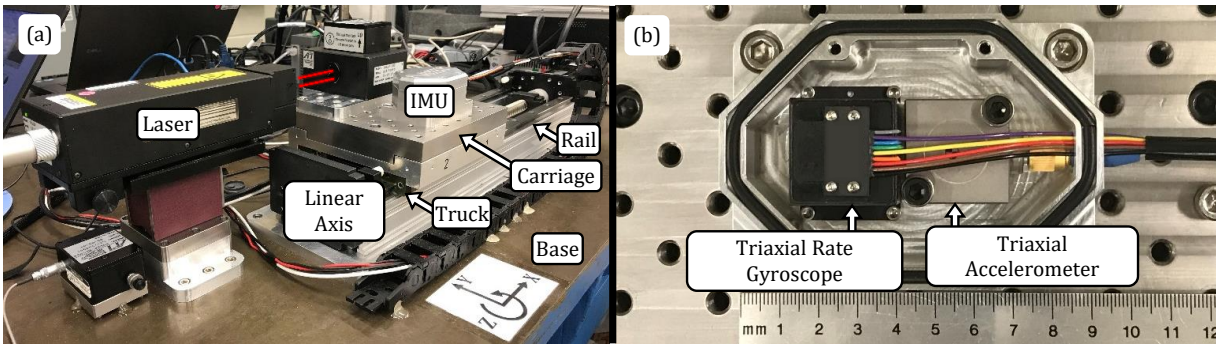

Figure 1. (a) Linear axis testbed, including linear axis, laser-based reference system, and IMU, and (b) top view of IMU without its lid.

Table 1
Specified properties of sensors used in the IMU.

Sensor	Bandwidth[a]	Noise
Accelerometer	0 Hz to 400 Hz	69 (µm/s^2)/√Hz
Rate Gyroscope	0 Hz to 200 Hz	35 (µrad/s)/√Hz

[a] frequencies correspond to half-power points, also known as 3 dB points

Experimental Setup

The testbed was used to test various degradation patterns via defects intentionally imparted on a rail of the linear axis. The parts of the system must be explained briefly to understand the experiment.

Figure 2 shows various views of the rail and carriage assembly elements of the linear axis. As seen in Figure 2a, the linear axis consists of two rails, Rail 1 and Rail 2, upon which rides four trucks, Truck 1, Truck 2, etc. The interaction of the trucks and the rails causes nominally linear motion of the carriage that carries the IMU and the reference sensor box for collection of performance data.

In this study, an inner raceway of the linear axis, seen highlighted in green in Figure 2a, was mechanically degraded to simulate spalling that can occur while a linear axis operates within machine tools. Figure 2b shows an example of rail degradation, in which the inner raceway of Rail 1 was ground down to have wear with a nominal depth of 50 µm (Figure 2c). The length of the degradation region was increased incrementally from a state of no degradation (Stage 1) to a state with a 75-mm-long degradation zone (Stage 15).

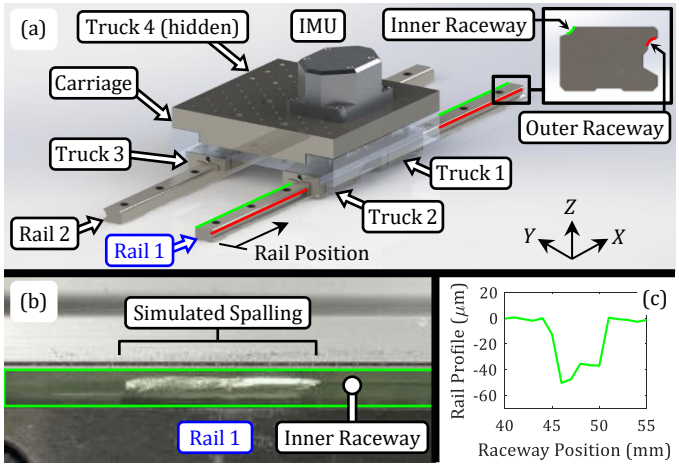

Figure 2. (a) Photorealistic view of rails and carriage assembly of one-axis testbed, (b) example of rail degradation and (c) its depth profile measured along the rail using a depth probe with a 3-mm-diameter sphere end.

With the overall system explained, some details of the system can now be understood. Figure 3b shows a zoomed-in front view of Rail 1 and Truck 2. Each rail has two raceway grooves upon which rides two recirculating ball loops from each truck, as denoted by the two dashed red circles in Figure 3b. The balls of the trucks interact with the raceway grooves to provide constraints for a single degree-of-freedom linear motion. However, any imperfections in this interaction create geometric error motions in six degrees of freedom. Therefore, as the balls and/or the raceway grooves deform (due to wear or other causes), the geometric performance of the carriage changes to reflect the degradation.

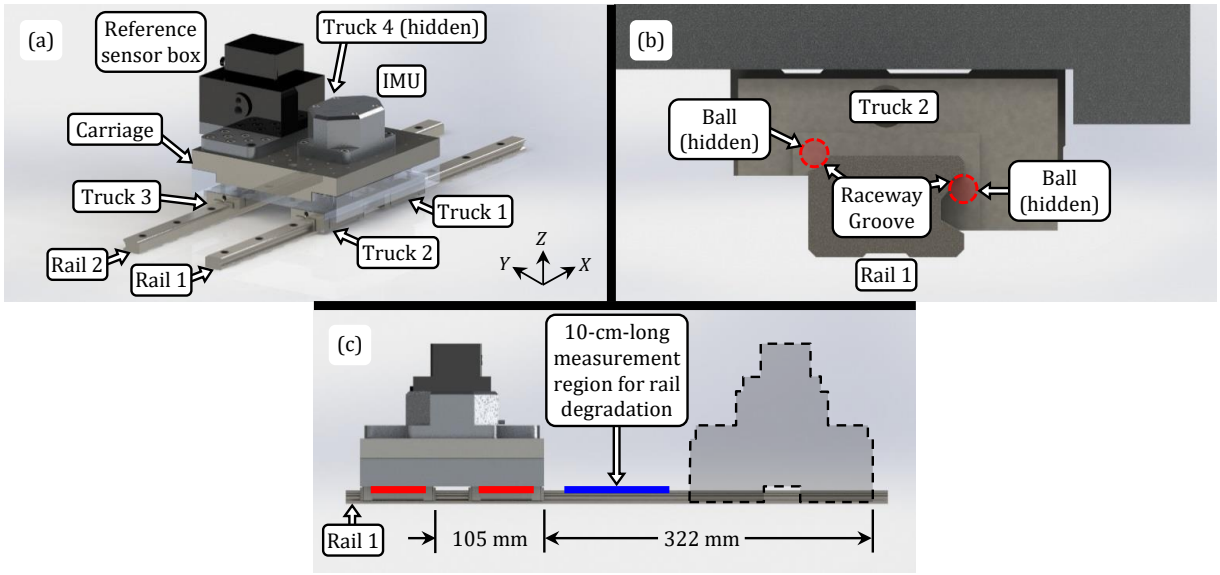

Figure 3. (a) Isometric view, (b) zoomed-in front view, and (c) side view of rails and carriage assembly, which includes four trucks, carriage, reference sensor box, and IMU, along with the interfaces where trucks interact with the rail degradation.

In this study, Rail 1 is intentionally degraded to various levels, affecting the carriage motion. Figure 3c shows a side view of Rail 1 and the carriage assembly. Rail 1 was degraded over a 10-cm-long region, as seen in Figure 3c. Thus, Truck 1 and Truck 2 interact with this region of the rail, changing the translational and angular error motions of the carriage. To mechanically simulate spalling, a handheld grinder was used to wear the surface of the raceway groove of Rail 1 seen in Figure 4a. The degradation zone length was increased incrementally by about 5.4 mm from its nominal state of no degradation, seen in Figure 4a, to its final state of significant degradation with a length of about 75 mm, seen in Figure 4c. Figure 4b shows the relative location and length of the degradation zone in the raceway groove for each of the fifteen (15) stages.

Of course, the rail degradation is three-dimensional and not just represented by a nominal length; each degradation zone has a depth profile experienced by each ball of a truck. Figure 5a shows the degradation profiles measured with a 3-mm-diameter probe, typically used for coordinate measuring machines, which was attached to a digital micrometer and fixed to the carriage for point-to-point measurements of the rail profile for all fifteen stages. The 'degradation' is defined here as the difference of a measured rail profile (e.g., for Stage 4) from the initial rail profile (for Stage 1). Hence, the degradation for Stage 1 is zero at all positions, as seen in Figure 5a. Also, as the degradation zone increases for each stage according to the schematic in Figure 4b, the degradation generally widens but maintains its nominal depth, as shown in Figure 5a. Accordingly, Figure 5b shows how the cumulative (integral) damage increases from 0 μm^2 to about 4 μm^2 (length $\times$ depth).

These measurements are used to corroborate and correlate the degradation estimations from the IMU-based results. However, it is worthwhile to note that the degradation profiles of Figure 5 are not true measurements of what the truck bearing balls experience. This results from two reasons. First, the probe diameter of 3 mm is slightly smaller than the bearing ball nominal diameter of 3.969 mm. Second, the micrometer measurements have uncertainties due to fixturing, thermal differences, etc. One sample (Stage 5) appears to be an outlier, likely caused by human error in fixturing. Regardless of this outlier, it appears that damage exists with depths greater than 50 µm.

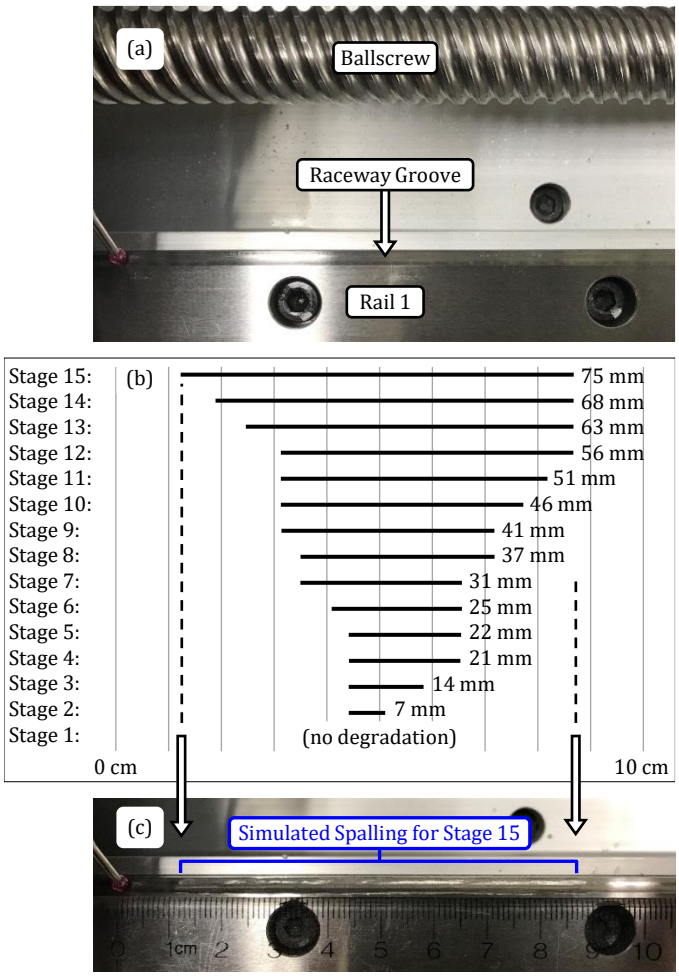

Figure 4. (a) Rail with no degradation, (b) schematic of relative location and length of degradation zone in raceway groove for each stage, and (c) rail with about 75 mm of 'spalling'. Degradations zones in (b) were measured within a 10-cm-long measurement region indicated by a ruler in (c).

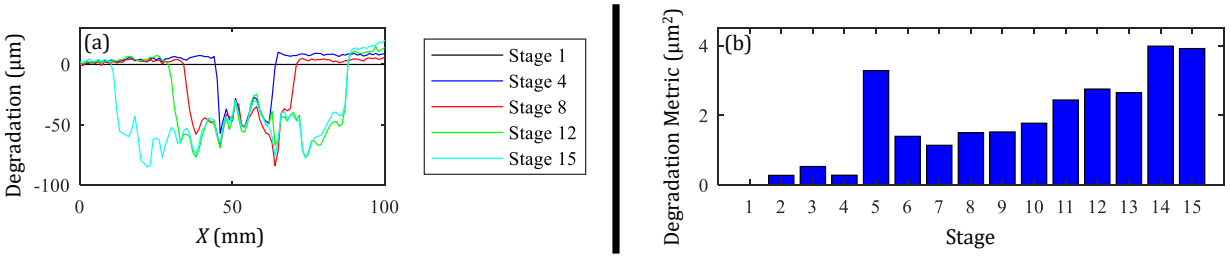

Figure 5. (a) Degradation profiles of the rail raceway groove for certain stages and (b) degradation metric for each stage.

Experimental Data Overview

Not only were micrometer measurements taken for each stage of degradation, but the IMU and laser-based reference data were also collected. For each stage, fifty (50) runs of IMU data were collected bidirectionally at slow (0.02 m/s), moderate (0.1 m/s), and fast (0.5 m/s) axis speeds, following the method described in Vogl et al. The axis position from the motor encoder was also collected simultaneously during each motion of the linear axis. Afterwards, ten (10) runs of laser-based reference data were collected bidirectionally at finite positions of travel, specifically every 1 mm between travel positions 1 mm and 321 mm. Even though the IMU and reference data are neither collected simultaneously nor measure the same errors (the IMU measures inertial states, while the reference system measures relative differences), the 'reference' system is treated as such without the availability of other data for a more accurate comparison. Furthermore, the vector pointing from the Reference sensor box to the IMU (see Figure 3a) is {ΔX, ΔY, ΔZ} = {0.015 m, -0.106 m, -0.015 m}.

Experimental Data Folders

There are fifteen (15) data folders, one for each stage of degradation. Each folder contains micrometer data, reference data, sensor box data (IMU and motor encoder data), as well as pictures. The format for each folder is as follows:

Date (20170418 to 20170518)

- Test 01
    - Micrometer Data
        - Micrometer Data.xlsx
    - Pics
        - Pictures of Micrometer Data collection
    - Reference Data
        - Screenshot of Reference Data (*.jpeg)
        - API 6DLSP data (API_6DLSP.ang, API_6DLSP.pos, and API_6DLSP.str)
        - API 6DLSP setup file (*.dst)
    - Sensor Box Data
        - Axis Under Test (X)
            - Axis Motion Direction (Positive or Negative)
                - Run Number (Run 01 to Run 50)
                - Axis Speed (Fast, Moderate, or Slow)
                - Data (Accelerometers.txt, Position.txt, Rate Gyroscopes.txt)

Reference Data Formats

For any given stage of degradation, the Reference Data is outputted as three files that have the following data formats with units, where E_{XX} denotes the linear positioning error motion of the X-axis, E_{YX} denotes the straightness error motion in the Y-direction, E_{ZX} denotes the straightness error motion in the Z-direction, E_{AX} denotes the angular error motion around the X-axis (roll), E_{BX} denotes the angular error motion around the Y-axis (pitch), and E_{CX} denotes the angular error motion around the Z-axis (yaw):

API_6DLSP.ang

X-position (mm)	$-E_{CX}$ (mrad)	E_{BX} (mrad)	$-E_{AX}$ (mrad)

API_6DLSP.pos

X-position (mm)	E_{XX} (mm)

API_6DLSP.str

X-position (mm)	$-E_{YX}$ (mm)	E_{ZX} (mm)

Sensor Box Data Formats

The Sensor Box Data contains data collected from the triaxial accelerometer (Accelerometers.txt) in the IMU, the triaxial rate gyroscope (Rate Gyroscopes.txt) in the IMU, and the motor encoder (Position.txt). The three files for each group of Sensor Box Data, for any given run number and axis speed, have the following data formats with units:

Accelerometers.txt

Time (seconds)	X-acceleration (m/s^2)	Y-acceleration (m/s^2)	Z-acceleration (m/s^2)	Zero column

Rate Gyroscopes.txt

Time (seconds)	X-angular velocity (rad/s)	Y-angular velocity (rad/s)	Z-angular velocity (rad/s)	Temperature (°C)

Position.txt

Time (seconds)	X-position (m)

Data Disclaimer

The National Institute of Standards and Technology (NIST) uses its best efforts to deliver a high-quality copy of the Database and to verify that the data contained therein have been selected on the basis of sound scientific judgment. However, NIST makes no warranties to that effect, and NIST shall not be liable for any damage that may result from errors or omissions in the Database.

Certain commercial entities, equipment, or materials may be identified in this document to describe an experimental procedure or concept adequately. Such identification is not intended to imply recommendation or endorsement by the National Institute of Standards and Technology (NIST), nor is it intended to imply that the entities, materials, or equipment are necessarily the best available for the purpose.